Wave-equation migration velocity analysis beyond the Born approximation

Paul Sava, Stanford University and Sergey Fomel, Lawrence Berkeley National Laboratory*

SUMMARY

Wavefield linearization using the Born approximation is based on the assumption of small slowness perturbation. We investigate the limits of the Born approximation when applied to wave-equation migration velocity analysis (WEMVA) and propose new schemes which allow for larger slowness anomalies, while enhancing accuracy and stability. The new schemes are based on linearizations of exponential functions using bilinear and implicit approximations. We demonstrate the feasibility of our new operators on a synthetic example with variable background and strong slowness anomalies.

INTRODUCTION

Migration methods using wavefield continuation techniques, commonly referred to as wave-equation methods, have enjoyed a renewed interest in the recent years, since the limitations of Kirchhoff migration became apparent (Geoltrain and Brac, 1993; Audebert et al., 1997; O'Brien and Etgen, 1998).

Migration velocity analysis based on downward continuation methods, also known as *wave-equation migration velocity analysis*, is a promising technique designed as a companion to wave-equation migration (Biondi and Sava, 1999). The main idea of WEMVA is to use downward continuation operators for migration velocity analysis (MVA), as well as for migration. This is in contrast with other techniques which use downward continuation for migration but traveltime-based techniques for migration velocity analysis (Clapp, 2001; Liu et al., 2001; Mosher et al., 2001).

WEMVA benefits from the same advantages over traveltime estimation methods as wave-equation migration benefits over Kirchhoff migration. The most important among them are the accurate handling of complex wavefields which are characterized by multipathing, and the band-limited nature of the imaging process, which can handle sharp velocity variations much better than traveltime-based methods (Woodward, 1992). Complex geology, therefore, is where WEMVA is expected to provide the largest benefits.

The problem we address in this paper is that, in its original form, WEMVA is based on wavefield linearization in the perturbation region using the Born approximation. This leads to severe limitations on the magnitude and size of the anomalies that can be resolved. This means that, in principle, it cannot operate successfully exactly in the regions of highest complexity.

In this paper, we introduce new methods of wavefield linearization designed to overcome the limitations imposed by the Born approximation. Our method is based on linearization of the exponential function containing the slowness perturbation, using more accurate approximations. The resulting operator is more accurate and also more stable in areas of high contrast. The cost is practically identical to that of the Born linearized operator.

DOWNWARD CONTINUATION MIGRATION

In migration by downward continuation, the wavefield at depth $z+\Delta z$, $\mathcal{W}(z+\Delta z)$, is obtained by phase-shift from the wavefield at depth z, $\mathcal{W}(z)$:

$$\mathcal{W}(z+\Delta z) = \mathcal{W}(z)\, e^{-ik_z \Delta z}. \tag{1}$$

This equation corresponds to the analytical solution of the ordinary differential equation

$$\frac{d}{dz}\mathcal{W}(z) = -ik_z \mathcal{W}(z). \tag{2}$$

Using a Taylor series expansion, the depth wavenumber (k_z) depends linearly on its value in the reference medium (k_{zr}) and the laterally varying slowness $s(x,y,z)$ in the depth interval under consideration

$$k_z \approx k_{zr} + \left.\frac{dk_z}{ds}\right|_{s=s_r} (s - s_r). \tag{3}$$

s_r represents the constant slowness associated with the depth slab between the two depth intervals. $\left.\frac{dk_z}{ds}\right|_{s=s_r}$ represents the derivative of the depth wavenumber with respect to the reference slowness and can be implemented in many different ways. Our choice is to implement it using the Fourier-domain method derived by Huang et al. (1999).

The wavefield downward continued through the *background* slowness $s_b(x,y,z)$ can be written using an expression similar to the one for the full wavefield as

$$\mathcal{W}_b(z+\Delta z) = \mathcal{W}(z)\, e^{-i\left[k_{zr} + \left.\frac{dk_z}{ds}\right|_{s=s_r}(s_b - s_r)\right]\Delta z}. \tag{4}$$

With this definition, the full wavefield $\mathcal{W}(z+\Delta z)$ depends on the background wavefield $\mathcal{W}_b(z+\Delta z)$ through the relation

$$\mathcal{W}(z+\Delta z) = \mathcal{W}_b(z+\Delta z)\, e^{-i\left.\frac{dk_z}{ds}\right|_{s=s_r}\Delta s \Delta z}, \tag{5}$$

where Δs represents the difference between the true and background slownesses $\Delta s = s - s_b$.

BORN WAVE-EQUATION MVA

Defining the *wavefield perturbation* $\Delta\mathcal{W}(z+\Delta z)$ as the difference between the wavefield propagated through the medium with correct velocity, $\mathcal{W}(z+\Delta z)$, and the wavefield propagated through the background medium, $\mathcal{W}_b(z+\Delta z)$, we can write

$$\begin{aligned} \Delta\mathcal{W}(z+\Delta z) &= \mathcal{W}(z+\Delta z) - \mathcal{W}_b(z+\Delta z) \\ &= \mathcal{W}_b(z+\Delta z)\left[e^{-i\left.\frac{dk_z}{ds}\right|_{s=s_r}\Delta s \Delta z} - 1\right]. \end{aligned} \tag{6}$$

Equation (6) represents the foundation of the wave-equation migration velocity analysis method (Biondi and Sava, 1999). The major problem with Equation (6) is that the wavefield $\Delta\mathcal{W}$ and slowness perturbations Δs are not linearly related. Therefore, for inversion purposes, we need to find a linearization of this equation around the reference slowness, s_r.

Biondi and Sava (1999) choose to linearize Equation (6) using the Born approximation ($e^{i\phi} \approx 1 + i\phi$). With this choice, the WEMVA Equation (6) becomes

$$\Delta\mathcal{W}(z+\Delta z) = \mathcal{W}_b(z+\Delta z)\left[-i\left.\frac{dk_z}{ds}\right|_{s=s_r}\Delta s \Delta z\right]. \tag{7}$$

The problem with the linearization in Equation (7) is its assumption of small phase perturbations

$$1 + i\phi \approx \lim_{\phi\to 0} e^{i\phi},$$

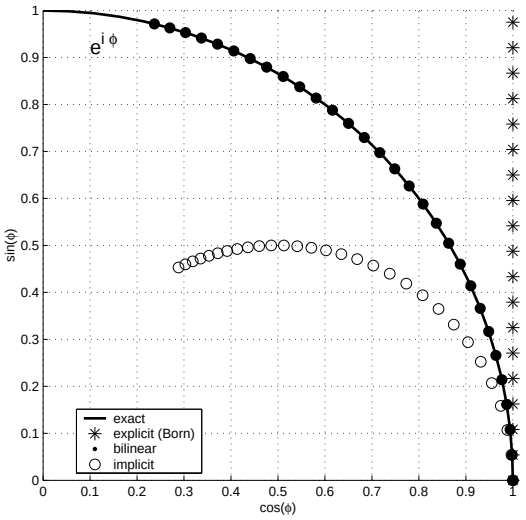

Figure 1: Explicit, bilinear and implicit approximations plotted on the unit circle, compared to the exact exponential solution.

which for our operator translates into small slowness perturbations. This fact is more apparent if we recall that this linearization corresponds to an explicit numerical solution of the differential equation (2), which is notoriously unstable unless we take small propagation steps.

The main consequence of the limitations imposed by the Born approximation is that WEMVA can only consider small perturbations in the slowness model, which are likely inadequate for real problems. Since non-linear inversion is still not feasible for the large sized problems typical for seismic imaging, we seek other ways of linearizing Equation (6) which would still enable inversion within the framework of linear optimization theory.

ALTERNATIVE LINEARIZATION

As noted earlier, the linear approximation as a function of the ϕ

$$e^{i\phi} \approx 1 + i\phi \tag{8}$$

corresponds to an *explicit* numerical solution to the differential equation (2). However, this is neither the only possible solution nor the most accurate. Furthermore it is only conditionally stable.

We can, however, solve Equation (2) using other numerical schemes. Two possibilities are *implicit* and *bilinear* numerical solutions, where we approximate respectively

$$e^{i\phi} \approx \frac{1}{1-i\phi}, \tag{9}$$

$$e^{i\phi} \approx \frac{2+i\phi}{2-i\phi}. \tag{10}$$

In the context of partial differential equations, the bilinear approximation (10) is known under the name of Crank-Nicolson method and has been extensively used in migration by downward continuation using the paraxial wave equation (Claerbout, 1985). Figure 1 compares the approximations in Equations (8), (9) and (10) as a function of the complex phase $i\phi$. Both the explicit and implicit solutions are characterized by amplitude and phase errors, while the bilinear solution leads just to phase errors.

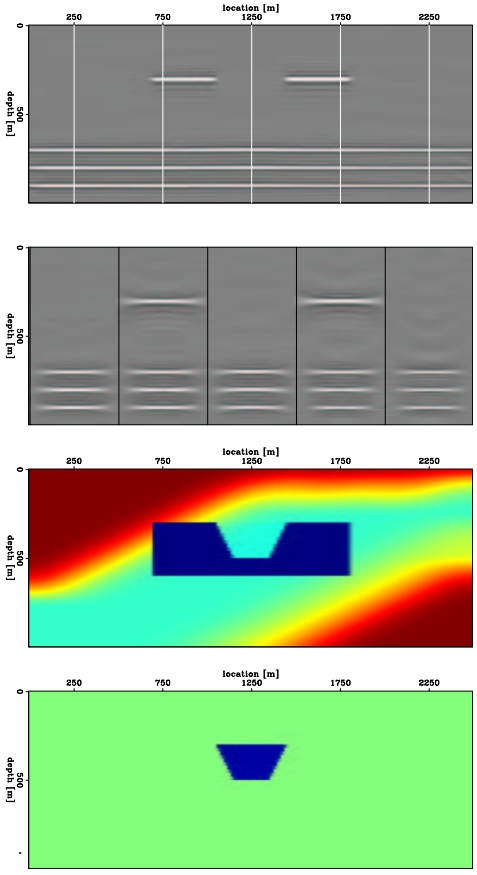

Figure 2: Synthetic model. Reflectivity model and a few angle-gathers corresponding to the vertical grid in the upper plot (top two panels). Background slowness model and slowness perturbation (bottom two panels).

To simplify Equation (6), we define $\beta = -i \left.\frac{dk_z}{ds}\right|_{s=s_r} \Delta z$, and so the WEMVA equation becomes

$$\Delta \mathcal{W} = \mathcal{W}_b \left[e^{\beta \Delta s} - 1 \right]. \tag{11}$$

The linearizations corresponding to the explicit, bilinear and implicit solutions respectively are

$$\begin{aligned} \Delta \mathcal{W} &\approx \mathcal{W}_b \beta \Delta s \\ &\approx \mathcal{W}_b \frac{2\beta \Delta s}{2-\beta \Delta s} \\ &\approx \mathcal{W}_b \frac{\beta \Delta s}{1-\beta \Delta s}. \end{aligned} \tag{12}$$

Apparently, just the first equation in (12) provides a linear relationship between $\Delta \mathcal{W}$ and Δs. However, a simple re-arrangement of terms in each leads to

$$\begin{aligned} \Delta \mathcal{W} &\approx \beta [\mathcal{W}_b] \Delta s \\ &\approx \beta \left[\mathcal{W}_b + \frac{1}{2} \Delta \mathcal{W} \right] \Delta s \\ &\approx \beta [\mathcal{W}_b + \Delta \mathcal{W}] \Delta s. \end{aligned} \tag{13}$$

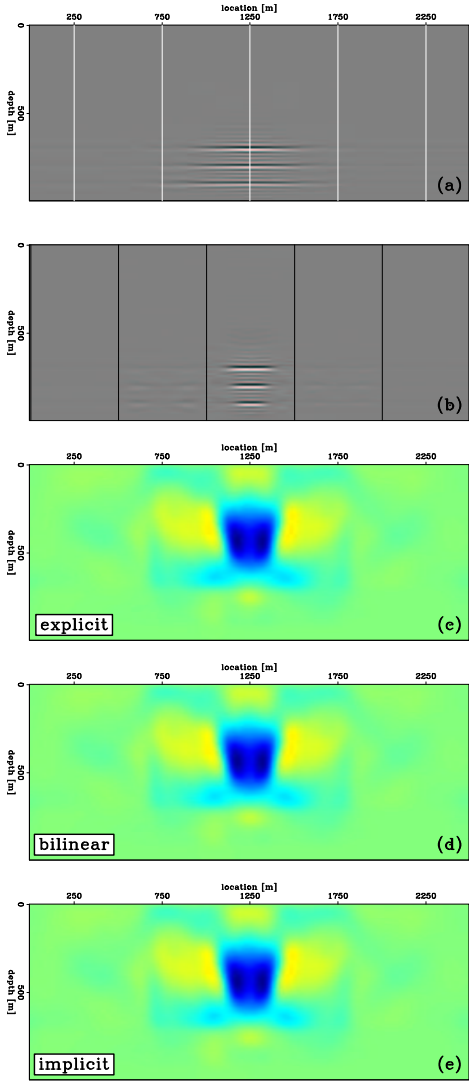

Figure 3: Slowness anomaly of 1% relative to the background. From top to bottom: stacked image, angle-domain common image gathers, and inversion using the explicit, bilinear and implicit operators.

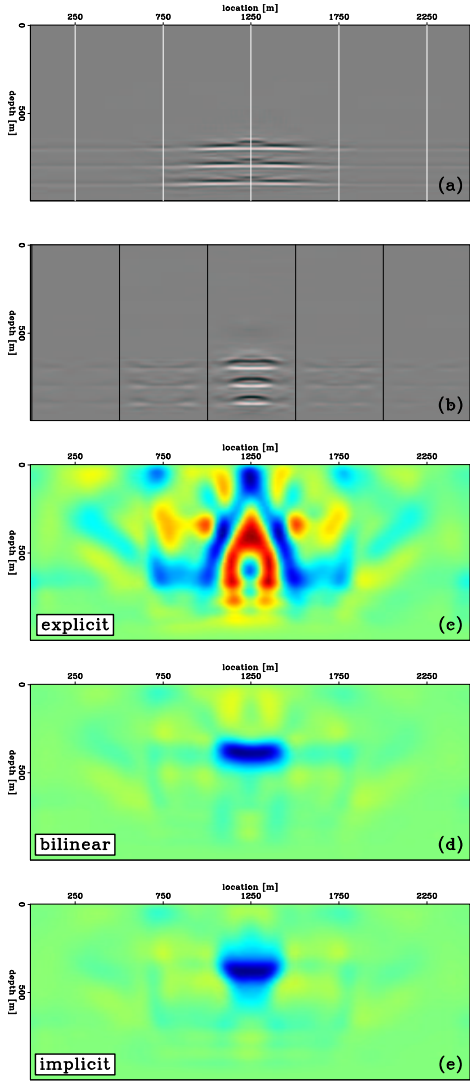

Figure 4: Slowness anomaly of 20% relative to the background. From top to bottom: stacked image, angle-domain common image gathers, and inversion using the explicit, bilinear and implicit operators.

For MVA, both the background ($\mathcal{W}_b$) and perturbation wavefields ($\Delta\mathcal{W}$) are known, so it is not a problem to incorporate them in the linear operator. In any of the cases described in Equation (13), the approximations can be symbolically described by the generic equation

$$\mathbf{d} \approx \mathbf{L}\mathbf{m}, \tag{14}$$

where the data $\mathbf{d}$ is the wavefield perturbation, and the model $\mathbf{m}$ is the slowness perturbation. The same operator $\mathbf{L}$ is used for inversion in all situations, and the only change is the wavefield that is fed into the linear operator. Therefore, the new operators are not more expensive than the Born operator.

All linear relationships in Equation (13) belong to a family of approximations of the general form

$$\Delta\mathcal{W} \quad \approx \quad \beta\,[\mathcal{W}_b + \xi\,\Delta\mathcal{W}]\,\Delta s, \tag{15}$$

where different members are obtained using appropriate values of the parameter $\xi \in [0,1]$. All forms of Equation (15), are approximations to the exact non-linear relation (11), therefore they are all likely to break for large values of the slowness perturbation or frequency. Nevertheless, these approximations enable us to achieve higher accuracy in slowness estimation as compared to the simple Born approximation.

The physical interpretation of the parameter ξ in Equation (15) is that of fraction of the depth step (Δz) inside any given depth slab where we linearize the known wavefields from its top and bottom with respect to the background slowness. For example, $\xi = 0, \frac{1}{2}, 1$ correspond respectively to linearizations at the bottom, middle and top of the slab. The case of $\xi = 0$ corresponds to the Born method, while $\xi = 1$ resembles what is known in the scattering literature as *wavefield renormalization* (Wang, 1997), when the entire wavefield and not only the background wavefield is involved in scattering.

Finally, we note that Equation (15) cannot be used for forward modeling of the wavefield perturbations $\Delta\mathcal{W}$, except for the particular case $\xi = 0$, since the output quantity is contained in the operator itself. However, we can use this equation for inversion for any choice of the parameter ξ.

EXAMPLES

We demonstrate the technique outlined in the preceding section using a synthetic example. The model (Figure 2) consists of a high velocity body incorporated in a background with strong but smooth lateral velocity variation.

Our example shows the results of inversion for a regularized problem which is symbolically summarized by the fitting goals:

$$\Delta R \approx \mathbf{L}\Delta s \tag{16}$$

$$0 \approx \mathbf{A}\Delta s, \tag{17}$$

where ΔR is the image perturbation related to the wavefield perturbation $\Delta\mathcal{W}$ through an imaging condition. Δs is the corresponding slowness perturbation, $\mathbf{L}$ is one of the linearized WEMVA operators in Equation (15) and $\mathbf{A}$ is a roughening operator.

In practice, image perturbations are created by taking the difference between an image created using a reference slowness model, and an improved version of it. Improved images can be generated by residual moveout, residual migration, or by any other procedure which improves images. For our experiments, we generate the image perturbation by taking the difference between two images created using two slowness models ($\Delta R = R - R_o$), which may be regarded as the ideal image perturbation.

We analyze several cases where we change the anomaly magnitude from 1% to 50% of the background slowness, but keep its shape unchanged. In Figures 3 and 4, we present two cases corresponding to anomalies of 1% and 20%.

In both Figures 3 and 4, panels (a) and (b) show the image perturbations created by the slowness anomalies. Panels (a) are stacked images and panels (b) are angle-domain common image gathers (Sava et al., 2001) corresponding to the vertical lines in the stack panels.

Panels (c), (d), and (e) of Figures 3 and 4 show the inverted slowness perturbations corresponding to the linearizations in Equation (13).

For the case of small slowness perturbation (Figure 3), the images we are subtracting are not too different from each-other. Therefore, we do not violate the Born approximation and consequently, inversion with either of the linear operators described in this paper, converge to an anomaly very close to our model.

The case of the much larger slowness perturbation (Figure 4) is different. We are subtracting images that are far from each-other and so we violate the Born approximation. Panels (a) and (b) show that portions of the reflectors we are comparing are so far from each-other that they are not even in direct contact. Consequently, inversion using the Born operator, panel (a), does not converge to a meaningful slowness perturbation. However, the bilinear and implicit approximations, panels (d) and (e), perform better. Both are still stable and allow the inversion to converge to slowness perturbations of correct shape.

CONCLUSIONS

In this paper, we investigate the limits of the Born approximation when applied to wave-equation migration velocity analysis. We find that the Born approximation is only valid for small slowness anomalies, on the order of $1-2\%$ of the background slowness for an anomaly of the shape and size used in the example in this paper. These numbers, however, are model dependent, because we have to consider both the magnitude and size of the anomaly: a small anomaly of large magnitude can have a similar effect as a large anomaly of small magnitude.

Improved WEMVA operators are needed to move beyond the Born approximation and better handle the non-linearity of image perturbations. We propose new versions of the WEMVA operator which are more appropriate for the case of large/strong slowness anomalies. Our new operators involve linearization using bilinear and implicit approximations to the exponential function. With the new operators, we not only improve accuracy but we also maintain stability of the inversion scheme at much higher values of the slowness anomalies.

Finally, we note that our new operators come at practically no additional cost compared with the Born-linearized operator. Importantly, they improve both the accuracy and stability of wave-equation migration velocity analysis.

REFERENCES

Audebert, F., Nichols, D., Rekdal, T., Biondi, B., Lumley, D. E., and Urdaneta, H., 1997, Imaging complex geologic structure with single-arrival Kirchhoff prestack depth migration: Geophysics, **62**, no. 05, 1533–1543.

Biondi, B., and Sava, P., 1999, Wave-equation migration velocity analysis: 69th Ann. Internat. Meeting, Soc. Expl. Geophys., Expanded Abstracts, 1723–1726.

Claerbout, J. F., 1985, Imaging the Earth's Interior: Blackwell Scientific Publications.

Clapp, R. G., 2001, Geologically constrained migration velocity analysis: Ph.D. thesis, Stanford University.

Geoltrain, S., and Brac, J., 1993, Can we image complex structures with first-arrival traveltime?: Geophysics, **58**, no. 04, 564–575.

Huang, L., Fehler, M. C., and Wu, R. S., 1999, Extended local Born Fourier migration method: Geophysics, **64**, no. 5, 1524–1534.

Liu, W., Popovici, A., Bevc, D., and Biondi, B., 2001, 3-D migration velocity analysis for common image gathers in the reflection angle domain: 71st Annual Internat. Mtg., Soc. Expl. Geophys., Expanded Abstracts, 885–888.

Mosher, C., Jin, S., and Foster, D., 2001, Migration velocity analysis using angle image gathers: 71st Annual Internat. Mtg., Soc. Expl. Geophys., Expanded Abstracts, 889–892.

O'Brien, M. J., and Etgen, J. T., 1998, Wavefield imaging of complex structures with sparse point-receiver data: 68th Annual Internat. Mtg., Soc. Expl. Geophys., Expanded Abstracts, 1365–1368.

Sava, P., Biondi, B., and Fomel, S., 2001, Amplitude-preserved common image gathers by wave-equation migration: 71st Ann. Internat. Mtg., Soc. Expl. Geophys., Expanded Abstracts, 296–299.

Wang, G. Y., 1997, Wave scattering and diffraction tomography in complex media: Ph.D. thesis, Stanford University.

Woodward, M. J., 1992, Wave-equation tomography: Geophysics, **57**, no. 01, 15–26.